Development of fractal geometry in a one-dimensional gravitational system Développement de la géométrie fractale dans un système gravitationnel à une dimension

Bruce N. Miller, Jean-Louis Rouet

Development of Fractal Geometry in a One Dimensional Gravitational System

Bruce N. Miller *

Department of Physics and Astronomy, Texas Christian University, Fort Worth, Texas 76129

Jean-Louis Rouet

Institut des Sciences de la Terre d'Orléans (ISTO) UMR6113 CNRS/Université d'Orléans 1A, rue de la Férollerie 45071 Orléans Cedex 2 et Laboratoire de Mathématique, Applications et Physique Mathématique - UMR 6628, Université d'Orléans, UFR des Sciences, F-45067 Orléans Cedex 2, France

Abstract

We study a one dimensional model of gravitational instability in a matter dominated universe. Careful scaling in both space and time results in an N-body problem governed by an autonomous set of coupled equations for the evolution of the system in phase space. Using dynamical simulation, we demonstrate that the system exhibits hierarchical structure formation. In common with galaxy observations, careful analysis suggests that, as time evolves, the distribution of particle positions develops bifractal geometry.

Key words: gravity, fractal, cosmology, hierarchical structure
PACS: 05.10.-a, 05.45.-a, 98.65.-r, 98.80.-k

* Corresponding author. Address: Department of Physics and Astronomy, Texas Christian University, Fort Worth, Texas 76129
Email addresses: b.miller@tcu.edu (Bruce N. Miller), jean-louis.rouet@univ-orleans.fr (Jean-Louis Rouet).
URL: http://personal.tcu.edu/ bmiller (Bruce N. Miller).

[1] The authors benefitted from the support of the division of Information Services and the Research Foundation of Texas Christian University. They also benefitted from computational assistance provided by E.Leguirriec. B.Miller is grateful for support received from the Université d'Orléans.

1 Introduction

In the last few decades dynamical N body simulation of cold dark matter (CDM) has experienced rapid advances due to improvements in both algorithms and technology.[2, 4] It is now possible to carry out gravitational N body simulations with upwards of 10^7 point mass particles. However, in order to employ simulation methods for systems evolving over cosmological time it is necessary to compromise the representation of the gravitational interaction over both long and short length scales. For example, tree methods are frequently employed for large separations, and it is typical to compute the gravitational field from a grid and introduce a short range cut-off to control the short-range singularity in the Newtonian pair potential. [2, 4] Unfortunately, even if the simulations were perfect, a system of even 10^9 particles provides only 10^3 particles per dimension and would thus be insufficient to investigate the fractal geometry with confidence.

As a logical consequence of these difficulties it was natural that physicists would look to lower dimensional models for insight. Although this sacrifices the correct dynamics, it provides an arena where accurate computations with large numbers of particles can be carried out for significant cosmological time. It is hoped that insights gained from making this trade off are beneficial. In one dimension, Newtonian gravity corresponds to a system of infinitesimally thin, parallel, mass sheets of infinite spatial extent. Since there is no curvature in a 1+1 dimensional gravitational system, we cannot expect to obtain equations of motion from general relativity. Then a question arises concerning the inclusion of the Hubble flow into the dynamical formulation. This has been addressed in two ways. In the earliest studies, carried out by Rouet et. al., the scale function was directly inserted into the one dimensional dynamics.[16, 17] Alternatively, starting with the usual three dimensional equations of motion and embedding a stratified mass distribution, Fanelli and Aurell obtained a similar set of coupled differential equations for the evolution of the system in phase space.[6] However, it was necessary to adjust the background contribution to account for the difference in dimension. While the approaches are different, from the standpoint of mathematics the two models are very similar and differ only in the values of a single fixed parameter. Following Fanelli, we refer to the former as the RF model and the latter as the Quintic, or Q, model.

By introducing scaling in both position and time, in each model autonomous equations of motion are obtained in the comoving frame. In addition to the contribution from the gravitational field, in each model there is now a background term corresponding to a constant negative mass distribution, and a linear friction term. By eliminating the friction term a Hamiltonian version can also be constructed. At least three other one dimensional models have also been investigated, one consisting of Newtonian mass sheets which

stick together whenever they cross,[10] one evolved by directly integrating the Zeldovich equations,[18, 19] and the continuous system satisfying Burger's equation[8]. In addition, fractal behavior has been studied in the autonomous one dimensional system where there is no background Hubble flow.[11, 12]

In dynamical simulations, both the RF and Quintic model clearly manifest the development of hierarchical clustering in both configuration and μ space (the projection of the phase space on the position-velocity plane). In common with the observation of galaxy positions, as time evolves both dense clusters and relatively empty regions (voids) develop. In their seminal work, by computing the box counting dimension for the RF model, Rouet et. al. were able to directly demonstrate the formation of fractal structure.[16, 17] They found a value of about 0.6 for the box counting dimension of the well evolved mass points in the configuration space, indicating the formation of a robust fractal geometry. In a later work, Miller and Rouet investigated the generalized dimension of the RF model.[5] In common with the analysis of galaxy observations by Balian and Schaeffer [3] they found evidence for bifractal geometry. Although they did not compute actual dimensions, Fanelli et. al. also found a suggestion of bifractal behavior in the model without friction.[1] It is then not surprising that the autonomous, isolated, gravitational system that does not incorporate the Hubble flow also manifests fractal behavior for short times as long as the virial ratio realized in the initial conditions is very small.[11, 12] In addition, in the one dimensional model of turbulence governed by Burger's equation, the formation of shocks has the appearance of density singularities that are similar to the clusters found in the RF and Quintic model. A type of bi-fractal geometry has also been demonstrated for this system.[8]

Below we present the results of our recent investigation of multi-fractal properties of the Quintic model. In section two we will first describe the system. Then we will outline a derivation of the equations of motion and explain how they differ from the other models mentioned above. In section three we will explain how the simulations were carried out and describe their qualitative features. In section four we define the generalized dimension and other fractal measures, present our approach for computing them, and present the results of the multi-fractal analysis. Finally conclusions will be presented in section five.

2 Description of the System

We are interested in the development of density fluctuations following the time of recombination. For that, and later, epochs, the Hubble expansion has slowed sufficiently that Newtonian dynamics provides an adequate representation of the motion in a finite region. Then, in a $3+1$ dimensional universe,

the Newtonian equations governing a mass point are simply

$$\frac{d\mathbf{r}}{dt} = \mathbf{v}, \qquad \frac{d\mathbf{v}}{dt} = \mathbf{E}_g(\mathbf{r},t) \tag{1}$$

where $\mathbf{E}_g(\mathbf{r},t)$ is the gravitational field. We wish to follow the motion in a frame of reference where the average density remains constant, i.e. the comoving frame. We also want to scale the time in order to eliminate explicit time dependence in the evolution equations. We introduce functions $A(t)$ and $B(t)$; $A(t) = \left(\frac{t}{t_o}\right)^{\frac{2}{3}}$, $\quad B(t) = \frac{t}{t_o}$, and transform space and time according to $\mathbf{r} = A(t)\mathbf{x}$, $dt = B(t)d\tau$. The choice of $A(t)$ gives the expansion factor for a matter dominated universe [15] with density $\rho_b(t) = (6\pi G t^2)^{-1}$. In the above t_o is some arbitrary initial time corresponding, say, to the epoch of recombination, G is the universal gravitational constant, and $\rho_b(t)$ is the average, uniform, density frequently referred to as the background density. Since the average Hubble flow is uniform, we note that $\rho_b(t_o) = A(t)^3\rho_b(t)$ and, as a result of the inverse square law for the gravitational field, $\mathbf{E}_g(\mathbf{r},t = A^2\mathbf{E}_g(\mathbf{x},t)$ where the functional dependence is preserved. Consideration of the above reduces the equations of motion to

$$\frac{d^2\mathbf{x}}{d\tau^2} + \frac{1}{3t_0}\frac{d\mathbf{x}}{d\tau} - \frac{2}{9t_0^2}\mathbf{x} = \mathbf{E}_g(\mathbf{x}) \tag{2}$$

which now includes both a linear friction (second term) and a negative background density (third term).

For the special case of a stratified mass distribution, from symmetry the gravitational field only has a component in the x direction. Moreover, the gravitational field at particle i is proportional to the difference between the mass/area on its right, i.e. due to sheets with $x_j > x_i$, and its left. The correct form of the gravitational field occurring on the right hand side of equation 2 at the location of particle i is then

$$E_g(x_i) = 2\pi m(t_0)G[N_{R,i} - N_{L,i}] \tag{3}$$

where $N_{R,i}$ ($N_{L,i}$) is the number of particles (sheets) to its right (left), and we have noted that $m_j(t) = m(t_0)/A^2$. Let us assume that we have $2N$ particles (sheets) confined within a slab with width $2L$, i.e. $-L < x < L$. Then $\rho_b(t_o) = (6\pi G t_o^2)^{-1} = \left(\frac{N}{L}\right) m(t_o)$ and the equation of motion for a particle in the system can be written

$$\frac{d^2x_i}{d\tau^2} + \frac{1}{3t_0}\frac{dx_i}{d\tau} - \frac{2}{3t_0^2}x_i = \frac{2}{3t_0^2}\left(\frac{L}{N}\right)[N_{R,i} - N_{L,i}]. \tag{4}$$

In obtaining the above we have adjusted the background term (third term on the left) so that it is equal to the field in the case of a uniform Hubble flow. This is necessary because of the change in dimension from 3+1 to 1+1. This is the Quintic model.

It is convenient to refer to Jean's theory for the final choice of units of time and length:

$$T_j = \omega_j^{-1} = (4\pi G\rho_b(t_o))^{-1/2} = \sqrt{\frac{3}{2}}t_o, \qquad \lambda_j = \sigma_v/\omega_j = \sqrt{\frac{3}{2}}\sigma_v t_o, \qquad (5)$$

where σ_v^2 is the variance of the velocity of the particles at the initial time. Then, with the further requirement that $L = n\lambda_j, \quad 0 < n < N$, and by measuring time and length in terms of these units, our equations become

$$\frac{d^2x_i}{d\tau^2} + \frac{1}{\sqrt{6}}\frac{dx_i}{d\tau} - x_i = \left(\frac{n}{N}\right)[N_{R,i} - N_{L,i}]. \qquad (6)$$

The description is completed by assuming that the system satisfies periodic boundary conditions on the interval $2L$.

3 Simulations

An attraction of these one-dimensional gravitational systems is their ease of simulation. In both the autonomous and RF models it is possible to integrate the motion of the individual particles between crossings analytically. Then the temporal evolution of the system can be obtained by following the successive crossings of the individual, adjacent, particle trajectories. This is true as well for the Q model. If we let $y_i = x_{i+1} - x_i$, where we have ordered the particle positions in the direction of increasing x, then we see the differential equation for each y_i is the same. By equating the general solution to zero we easily obtain a fifth order algebraic equation in $u = \exp(\tau/\sqrt{6})$. Hence the name Quintic model. These can be solved numerically in terms of the initial conditions by analytically bounding the roots and employing the Newton-Raphson method.

Typical numerical simulations were carried out for a system of $N = 2^{18}$ particles with $n = 3547$ Jean's lengths, λ_j. Initial conditions were chosen by equally spacing the particles on the line and randomly choosing their velocities from a uniform distribution within a fixed interval (waterbag). Other initial conditions, such as Normally distributed velocities, as well as a Brownian motion representation, were also investigated. The simulations were carried forward for approximately fifteen dimensionless time units.

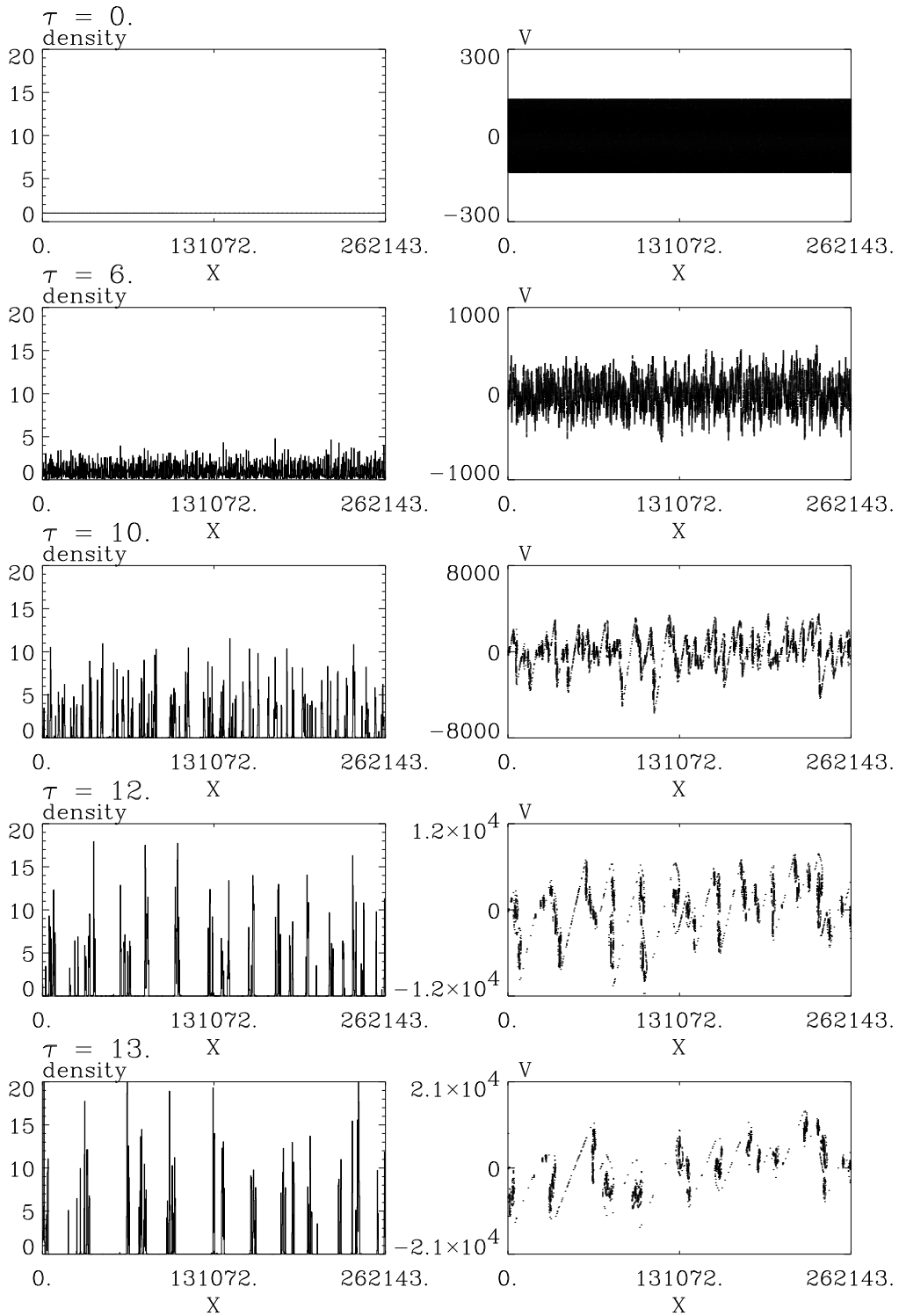

Fig. 1. Density and representation in *mu*-space for $\tau = 0$, 6, 10, 12 and 13 for a system of 262143 particles. The units are such that the lenght of the system is $\sim$ 3547 Jean's lenght with $\sim$ 74 particles by Jean's lenght.

In Fig.1 we present a visualization of a typical run. (see Fig. 1). In the left

column we present a histogram of the particles positions at increasing time units, while on the right we display the particle location in μ (position, velocity) space. It is clear from the panels that hierarchical clustering is occurring, i.e. small clusters are joining together to form larger ones. The first clusters seem to appear at roughly $\tau = 4$ and there are many, while by $\tau = 10$ there are on the order of ten clusters. Qualitatively similar histories are obtained for the RF model and the model without friction, as well as for the different boundary conditions mentioned above. However, there are some subtle differences. Simulations have also been performed where the system size is less that the Jean's length. The results support the stability analysis in that hierarchical clustering is not observed.

4 Fractal Analysis

It is natural to assume that the apparently self similar structure which develops in the phase plane as time evolves has fractal geometry, but we will see that things aren't so simple. In their earlier study of the RF model, Rouet and Feix found a box counting dimension for the particle positions of about 0.6 for an initial waterbag distribution (uniform on a rectangle in the phase plane-see above) [17]. As far as we know, Balian and Schaeffer were the first to suggest that the distribution of galaxy positions are consistent with a bifractal geometry. [3] Since the structures which evolve are strongly inhomogeneous, to gain further insight we have carried out a multi-fractal analysis [9] in both the position coordinate and the phase plane. To accomplish this we partitioned each space into cells of length l. At each time of observation in the simulation, a measure $\mu_i = N_i(t)/N_T$ was assigned to cell i, where $N_i(t)$ is the population of cell i at time t and N_T is the total number of particles in the simulation. The generalized dimension of order q is defined by [9]

$$D_q = \frac{1}{q-1} \lim_{l \to 0} \frac{\ln C_q}{\ln l}, \quad C_q = \Sigma \mu_i. \tag{7}$$

where D_0 is the box counting dimension, D_1, obtained by taking the limit $q \to 1$, is the information dimension, and D_2 is the correlation dimension [9]. As q increases above 0, the D_q provides information on the geometry of cells with higher population.

In practice, it is not possible to take the limit $l \to 0$ with a finite sample. Instead, one looks for a scaling relation over a substantial range of $\ln l$ with the hope that a linear relation between $\ln C_q$ and $\ln l$ occurs, suggesting power law dependence of C_q on l. Then, in the most favorable case, the slope of the linear region should provide the correct power and, after dividing by $q-1$, the

generalized dimension D_q. As a rule, or guide, if scaling can be found, either from experiment or computation, over three decades of l then we typically infer that there is good evidence of fractal structure.[13] Also of interest is τ_q, where $C_q \sim l^{\tau_q}$ for small l . τ_q and D_q are related to each other through a Legendre transformation [14]. Here we present the results of our fractal analysis of the particle positions on the line. It is well established by proof and example that, for a normal, homogeneous, fractal, all of the generalized dimensions are equal, while for an inhomogeneous fractal, e.g. the Henon attractor, D_q is a decreasing function of its argument.[9]

As time progressed, for the initial conditions discussed above, typically two independent scaling regimes developed. The size of each scaling range depended on both the elapsed time into the simulation and the value of q. While the length of each scaling regime varied with both q and time, it was possible to find good scaling over up to four decades in l!

In Fig. 2 we see a plot $\frac{1}{q-1}\ln C_q$ versus $\ln l$ for $q = -3$ at the time $T = 13$ for the simulation the results of which are given Fig. 1. We clearly observe a single large scaling range with a hint of some other behavior developing for $\ln l > 5$. Now let's increase the value of q. In Fig.3 we again plot $\frac{1}{q-1}\ln C_q$ versus $\ln l$ but now with $q = 2$. We see that the large scaling range has split into two smaller regions separated at about $\ln l = 2$, and that the slope of the region with larger l has decreased compared with the scaling region on its left. This behavior commences at about $q = 1$ and persists until $q = 10$, which represents the limit of our computations. Note that, as a rule, the scaling region with smaller l is more robust. In Fig.4 we provide combined plots of τ_q versus q for each scaling range. We observe that, for $q < 0$, they approximately overlap with a fixed value of $\tau_q \cong -0.9$. On the other hand, for $q > 0$, τ_q is increasing for each scaling range. The upper curve represents the smaller scaling range and appears almost linear. In contrast the lower curve, corresponding to the scaling region with larger l , seems to be composed of two linear elements and undergos a change in slope at approximately $q \cong 1$. We zoom in on this special range of q (see Fig. 4) and observe that it is apparently composed of two linear segments. In Fig. 5 we provide a combined plot of D_q versus q for each range. The behavior for $q < 0$ is expected, since here τ_q is nearly constant so the behavior is determined by the factor $1/(q-1)$.Once again, for $q < 0$ the two curves nearly coincide. However, for $q > 0$ things become more interesting. The upper curve, corresponding to the smaller scaling region, continues to increase until $q \cong 2$ and then very gradually decreases. In contrast, the lower curve, corresponding to the upper scaling region, has a peak at $q \cong 0$ and then decreases until it nearly levels off with a value of about 0.63.

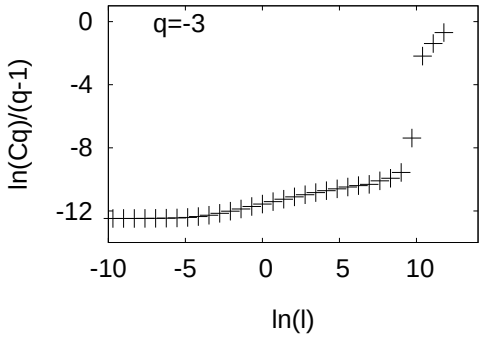

Fig. 2. $\ln(C_q)/(q-1)$ function of $\ln(l)$ for $q = -3$ at time 13. A scaling range could be observed, for $\ln(l) \in [-2.8; 6.2]$.

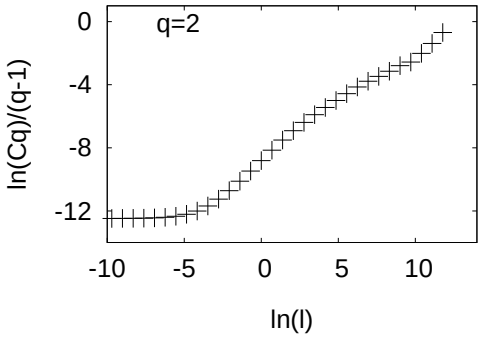

Fig. 3. $\ln(C_q)/(q-1)$ function of $\ln(l)$ for $q = 2$. Two scaling ranges could be observed, the first one for $\ln(l) \in [-2.8; 2.1]$, called SC1 hereafter, the second one for $\ln(l) \in [2.1; 6, 2]$, called SC2 hereafter.

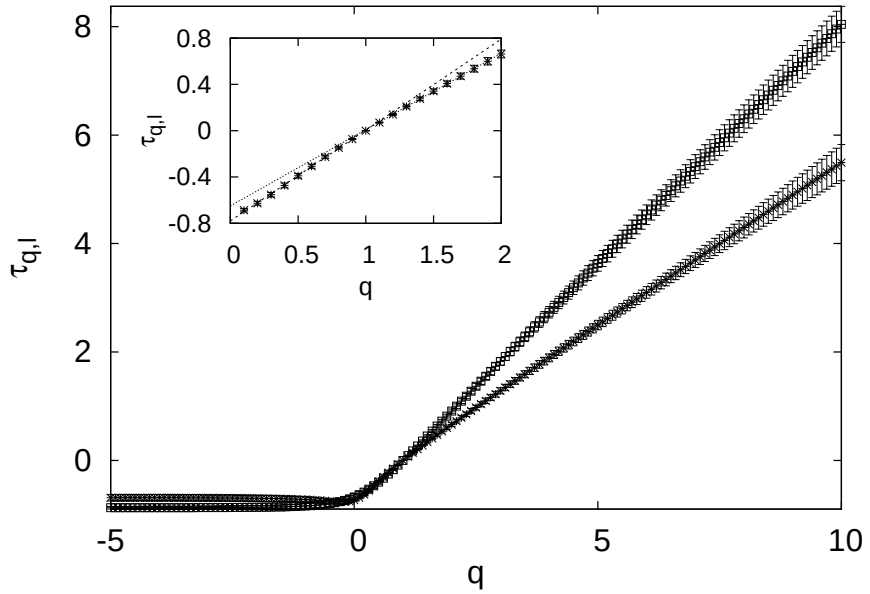

Fig. 4. $\tau(q,l) = (q-1)D(q,l)$ for the two scaling ranges SC1 (upper curve) and SC2 (lower curve) as defined figure 3 for q in the range $[-5, 10]$ by step of .1. The encapsulated figure is a zoom of τ_q for SC2 for $q \in [0, 2]$ showing two linear zones.

5 Discussion and Conclusions

As mentioned earlier, it is well established that, for a regular multifractal, the generalized dimension, D_q , is a decreasing function of its argument.[9] Therefore, for $q < 0$, it would be a stretch to interpret the simulation results as true generalized dimensions. There must be an alternative explanation for the behavior we observe. The picture for positive q is rather different: The two

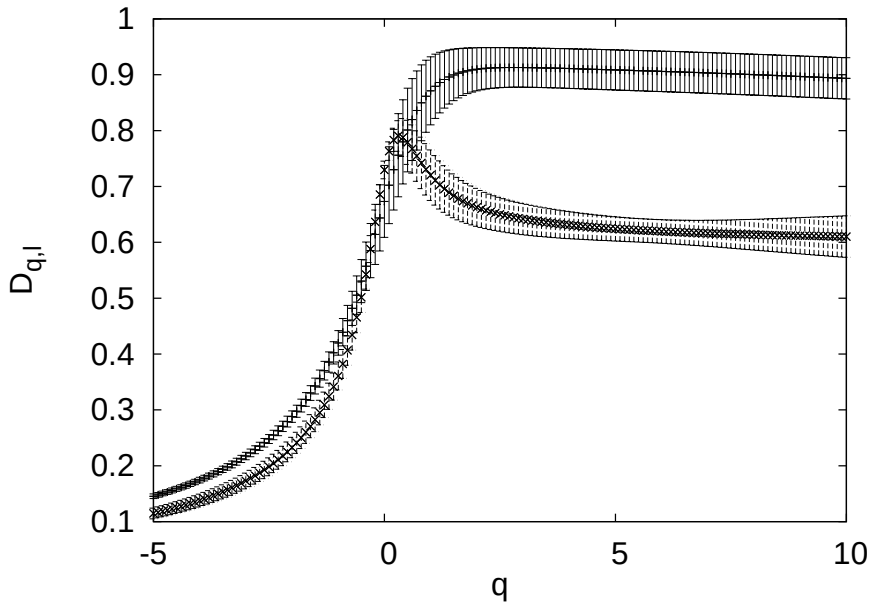

Fig. 5. $D(q, l)$ given by the slopes of the two scaling ranges SC1 (+) and SC2 (*) as defined figure 3 for q in the range $[-5, 10]$ by step of .1.

scaling regions give qualitatively different results. Although one would suspect from the definition of the generalized dimension that the scaling region with smaller l would give the correct result, this is hard to accept since the function is still increasing until $q = 2$. On the other hand, the second scaling region manifests a well behaved decreasing function which appears to approach a constant value of $D_q \cong 0.63$ for $q \lesssim 10$.

It is interesting that we have observed similar behavior with a well characterized, textbook, fractal that is discussed in numerous sources. As a test of our computational approach we simulated the multiplicative binomial process.[7] For this multifractal τ_q and D_q are known precisely.[7] When we carried out the fractal analysis using the methods described above, we also found two scaling regions. What is most striking is that the scaling region with larger values of l yielded a τ_q (and therefore D_q) which agreed to within numerical error with the theoretical prediction!

For $q > 0$ we seem to be seeing a similar phenomena in our simulations. Then how do we explain the surprising and counterintuitive results for $q < 0$? Since for negative q we obtain a nearly constant value for τ_q from each scaling region, it seems safe to assume that a region of the data characterized by a simple fractal behavior has the dominant influence. Moreover, since it only involves $q < 0$, it represents the regions of low density, i.e. the voids. Assuming monofractal behavior, we obtain $\tau_q = \alpha q - f(\alpha)$ where α is the strength of the local singularity, or the pointwise dimension, and $f(\alpha)$ is the dimension of its support.[14] Then the computations show that for $q < 0$ we must have $\alpha = 0$

and $f \cong 0.9$. This suggests that the results for negative q are dominated by regions of such low density that widely separated, "isolated", particles are responsible for the spurious behavior of D_q, i.e. they are an artefact. At this time this is simply a conjecture which needs to be investigated with further computation.

Finally let's consider in Fig.4 the plot of τ_q versus q for the larger scaling region (lower curve) with $q > 0$. As we mentioned earlier, for $0 < q < 1.5$ and for $2 < q < 10$ the curve appears linear with different slopes in each region. This may be the manifestation of bifractality first discussed by Balian and Schaeffer for galaxy positions. The first interval may represent the true fractal structure of the under-dense regions, while the dense clusters are dominant for the larger q values.

We have seen that one dimensional models develop hierarchical structure and manifest robust scaling behavior over particular length and time scales. In addition, they have an enormous computational advantage over higher dimensional models. It is possible to study the evolution of large systems with on the order of 200,000 particles per dimension and the evolution can be followed for relatively long times without compromising the dynamics. As a consequence, it is possible to study fractal geometry with some confidence.

In common with 3+1 dimensional cosmologies, with the inclusion of the Hubble expansion and the transformation to the comoving frame, both the 1+1 dimensional Quintic and RF models reveal the formation of dense clusters and voids. They also show evidence for bifractal geometry . This may be a consequence of dynamical instability that results in the separation of the system into regions of high and low density. An interesting observation is that the lower bound of the length scale that supports the trivial space dimension of unity grows with time. To the extent that similar behavior occurs in the 3+1 dimensional universe, this lends support for the standard cosmological model on large scales.

The system studied here shows evidence of two nontrivial scaling regions. The type of anomalous behavior of D_q and τ_q in the scaling region with smaller boxes was also found in the standard multiplicative binomial model with a similar sample size, suggesting that it is a finite size effect. This may also be true for the region of negative q where a fractal analysis forces us to conclude that the point-wise dimension vanishes. Computations with different initial conditions reveal similar behavior, but this work is only in the preliminary stages. Future work will include the analysis of fractal geometry in the μ (position, velocity) space, the computation of dimension from the correlation function, and the study of the properties of isolated under dense and over dense regions.

References

[1] E. Aurell, D. Fanelli, S. N. Gurbatov, and A. Y. Moshkov. *Physica D*, 186:171, 2003.

[2] J.S. Bagla. *Current Science*, 88:1088, 2005.

[3] R. Balian and R. Schaeffer. *Astronomy and Astrophysics*, 226:373, 1989.

[4] E. Bertschinger. *Annual Review of Astronomy and Astrophysics*, 36:599, 1998.

[5] B.N.Miller and J.-L. Rouet. *Physical Review E*, 65:056121, 2002.

[6] D. Fanelli and E. Aurell. *Astronomy and Astrophysics*, 395:399, 2002.

[7] Jens Feder. *Fractals*. Plenum, New York, 1988.

[8] S. N. Gurbatov, S. I. Simdyankin, U. Frisch E. Aurell, and G. Toth. 344:339, 1997.

[9] T. C. Halsey, M. H. Jensen, L. P. Kadanoff, I. Procaccia, and B. Shraiman. *Physical Review A*, 33:1141, 1986.

[10] L. A. Kofman, D. Pogosyan, S. F. Shandarin, and A. L. Melott. 393:437, 1992.

[11] H. Koyama and T. Konishi. *Physics Letters A*, 279:226, 2001.

[12] H. Koyama and T. Konishi. *Euro Physics Letters*, 58:356, 2002.

[13] J. L. McCauley. *Physica A*, 309:183, 2002.

[14] Ed Ott. *Chaos in Dynamical Systems*. Cambridge, Cambridge, UK, 2002.

[15] P. J. E. Peebles. *Principles of Physical Cosmology*. Princeton University Press, Princeton, NJ, 1993.

[16] J.-L. Rouet, M. R. Feix, and M. Navet. Fractals in astronomy. In A. Heck, editor, *Vistas in Astronomy 33*, pages 357–370. Pergamon, 1990.

[17] J.-L. Rouet, E. Jamin, and M. R. Feix. In A. Heck and J. M. Perdang, editors, *Applying Fractals in Astronomy*, pages 161–179. Springer-Verlag, Berlin, 1991.

[18] S. F. Shandarin and Ya. B. Zeldovich. *Reviews of Modern Physics*, 61:185, 1989.

[19] T. Tatekawa and K. Maeda. *Astrophysical Journal*, 547:531, 2001.